Plasmonic Supercrystals

Daniel García-Lojo,[1] Sara Nuñez-Sánchez,[1] Sergio Gómez-Graña,[1] Marek Grzelczak,[2,3] Isabel Pastoriza-Santos,[1] Jorge Pérez-Juste,[1*] and Luis M. Liz-Marzán[3,4 *]

[1] Department of Physical Chemistry and Biomedical Research Center (CINBIO), University of Vigo, Lagoas-Marcosende, 36310 Vigo, Spain

[2] Donostia International Physics Center (DIPC), Paseo Manuel de Lardizabal 4, Donostia – San Sebastián 20018, Spain

[3] Ikerbasque, Basque Foundation for Science, 48013 Bilbao, Spain

[4] CIC biomaGUNE and CIBER-BBN, Paseo de Miramón 182, 20014 Donostia-San Sebastián, Spain

CONSPECTUS: For decades, plasmonic nanoparticles have been extensively studied due to their extraordinary properties, related to localized surface plasmon resonances. A milestone in the field has been the development of the so-called seed-mediated growth method, a synthetic route that provided access to an extraordinary diversity of metal nanoparticles with tailored size, geometry and composition. Such a morphological control came along with an exquisite definition of the optical response of plasmonic nanoparticles, thereby increasing their prospects for implementation in various fields. The susceptibility of surface plasmons to respond to small changes in the surrounding medium or to perturb (enhance/quench) optical processes in nearby molecules, has been exploited for a wide range of applications, from biomedicine to energy harvesting. However, the possibilities offered by plasmonic nanoparticles can be expanded even further by their careful assembly into either disordered or ordered structures, in 2D and 3D. The assembly of plasmonic nanoparticles gives rise to coupling/hybridization effects, which are strongly dependent on interparticle spacing and orientation, generating extremely high electric fields (hot spots), confined at interparticle gaps. Thus, the use of plasmonic nanoparticle assemblies as optical sensors have led to improving the limits of detection for a wide variety of (bio)molecules and ions. Importantly, in the case of highly ordered plasmonic arrays, other novel and unique optical effects can be generated. Indeed, new functional materials have been developed *via* the assembly of nanoparticles into highly ordered architectures, ranging from thin films (2D) to colloidal crystals or supercrystals (3D). The progress in the design and fabrication of 3D supercrystals could pave the way toward next generation plasmonic sensors, photocatalysts, optomagnetic components, metamaterials, *etc*. In this Account, we summarize selected recent advancements in the field of highly ordered 3D plasmonic superlattices. We first analyze their fascinating optical properties, for various systems with increasing degrees of complexity, from an individual metal nanoparticle through particle clusters with low coordination numbers, to disordered self-assembled structures and finally to supercrystals. We then describe recent progress in the fabrication of 3D plasmonic supercrystals, focusing on specific strategies but without delving into the forces governing the self-assembly process. In the last section, we provide an overview of the potential applications of plasmonic supercrystals, with a particular emphasis on those related with surface-enhanced Raman scattering (SERS) sensing, followed by a brief highlight of the main conclusions and remaining challenges.

Introduction

A supercrystal can be defined as a highly ordered 3D assembly of nanocrystals/nanoparticles, which may still exhibit the intrinsic properties of its building blocks, but also displays unique collective properties originating from interparticle coupling effects.[1,2] By tuning the location, orientation, shape or composition of the nanoparticles, novel high-performance materials with custom-made properties can be created.[3-5] It is thus essential to properly understand particle crystallization processes, to rationalize and direct the formation of the desired supercrystals, in terms of symmetry, lattice spacing and even crystalline habit or shape. Such processes are complicated due to the wide range of nanoparticle interactions, as well as other experimental parameters involved (*e.g.* solvent, temperature, humidity).[2,6,7]

This Account focuses on plasmonic supercrystals and their potential use for diverse applications. We do not intend to discuss interparticle interactions, external forces or thermodynamics involved in the nanoparticle assembly process.[2,6] We will describe state-of-the-art techniques to fabricate highly ordered 3D plasmonic nanostructures comprising Au and Ag nanoparticles. By showing recent works including computational simulations and experimental data, we analyze the optical properties of plasmonic supercrystals, as well as the applicability of such plasmonic platforms.

Optical properties: Why plasmonic supercrystals?

Metal nanoparticles and films thereof have been extensively used as nanoprobes within sensing devices,[8] because of their ability to concentrate electric fields at the nanoscale, thereby enhancing the interaction between light and molecular analytes.[9,10] Plasmonic nanoparticle supercrystals can be foreseen as sensing platforms in either liquid or gaseous phase where the samples can flow between nanoparticles, where the electric field is strongly confined, thereby facilitating *e.g.* the analysis of clinical samples.[11,12] However, the fundamentals and design rules for optimum spatial distributions are not clear yet. We describe in this section recent literature where scientists from different areas attempted to define the fundamentals and basic design principles to develop supercrystals for enhanced spectroscopy applications. We first describe the optical response of single particles to gradually move into 3D nanoparticle arrays.

Localized surface plasmon resonances and hot spots

Nanometals have been the fuel for the nanosensing revolution due to their fascinating optical properties. In particular, metals having negative values of real permittivity can trap light at the metal-dielectric interface, coupling the electric field to free electrons in the metal, to form a hybrid surface wave named surface plasmon. For small nanoparticles, the electric field of incoming light can induce an electrical dipole through the displacement of conduction electrons from their equilibrium positions with respect to the core ions, resonating coherently with the incident light wave. This phenomenon is known as localized surface plasmon resonance (LSPR) and generates intense electric fields confined at the nanoparticle surface, which can alter certain properties (absorption, emission, Raman scattering, *etc*.) of nearby molecules.[13] Additionally, the plasmonic resonance frequency strongly depends on nanoparticle size, composition,[14] shape[15] and surrounding medium.[16] Therefore, the rational design and synthesis of plasmonic nanostructures is an attractive path to obtain more efficient sensing devices. As an example, nanoparticles containing spikes, *i.e.* nanostars, can strongly confine light at the tips of such spikes.[17,18]

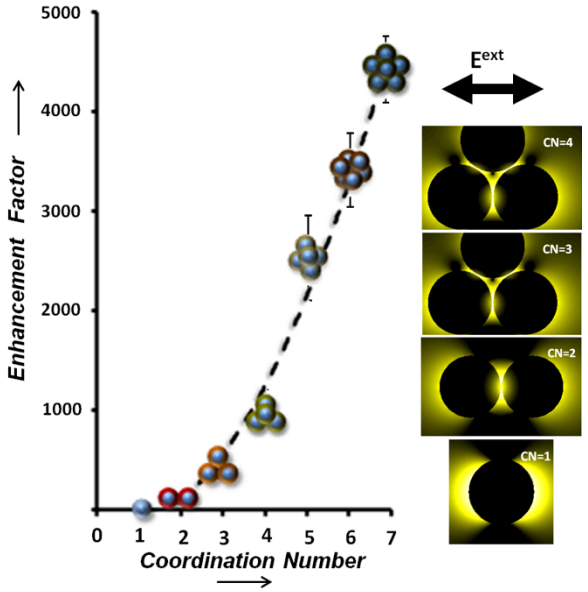

Figure 1. Comparison between SERS enhancement factors for clusters of spherical nanoparticles with coordination numbers 1 to 7, normalized to the enhancement by a single particle excited by a 633 nm laser line. Near field intensity calculated for clusters with low coordination numbers, excited at 633 nm, along planes passing by the centers of the lower spheres. Bright yellow areas correspond to hot spots. Adapted with permission from ref. 19. Copyright (2012) Wiley-VCH.

Assembly of nanoparticles into dimers, tetramers, clusters or chains has been shown to originate larger enhancement factors,[19,20] increasing by orders of magnitude with the number of assembled nanoparticles (**Figure 1**), in correlation with interparticle coupling. When two nanoparticles are close enough, individual plasmon resonances couple together generating hybridized plasmon modes.[21,22] Considering that a plasmonic nanoparticle can be described as a nanoantenna with an associated electric dipole,[23] when two nanoparticles are brought into close proximity their corresponding dipoles are hybridized, creating symmetric and antisymmetric plasmon modes, depending on their relative dipole orientations. The symmetric mode is due to coupling of mutually aligned longitudinal dipoles, leading to a large induced dipole. Symmetric modes are strongly coupled to the far field, which makes them radiative and therefore known as "bright" plasmons. On the other hand, antisymmetric hybrid modes stem from anti-aligned dipoles, resulting in no net dipole moment. Such modes cannot couple to the far field and are commonly known as "dark" plasmons. Both optical modes can generate extremely high local fields at nanogaps between nanoparticles, called hot spots (**Figure 1**),[19] which are considered the best positions to place a target analyte for efficient sensing.

The relationship between cluster size and optical properties has also been studied through solvent-induced self-assembly of 20 nm polystyrene-stabilized gold nanoparticles.[24] Gold nanoparticles in THF gradually aggregate upon water addition, producing stable clusters

upon introduction of a copolymer comprising polystyrene and poly(acrylic acid) blocks (PS-b-PAA). The authors observed that by increasing the length of grafted polystyrene (7, 17, 38 nm) the final cluster diameter also increased (49, 146, 270 nm) (**Figure 2A**). This trend was explained by hydrophobic forces driving clustering, which are closely related to the molecular weight of grafted polymer. Cluster size in turn affects the optical response, the LSPR redshifting further for larger diameters (number of particles per cluster) (**Figure 2B**). Structurally, electron tomography analysis revealed that the clusters display multi-shell structures with well-defined distances between concentric layers (**Figure 2C**).[25] This configuration was numerically confirmed by implementing the length of polymer chains and diameter of gold nanoparticles into pairwise attractive and repulsive interactions.

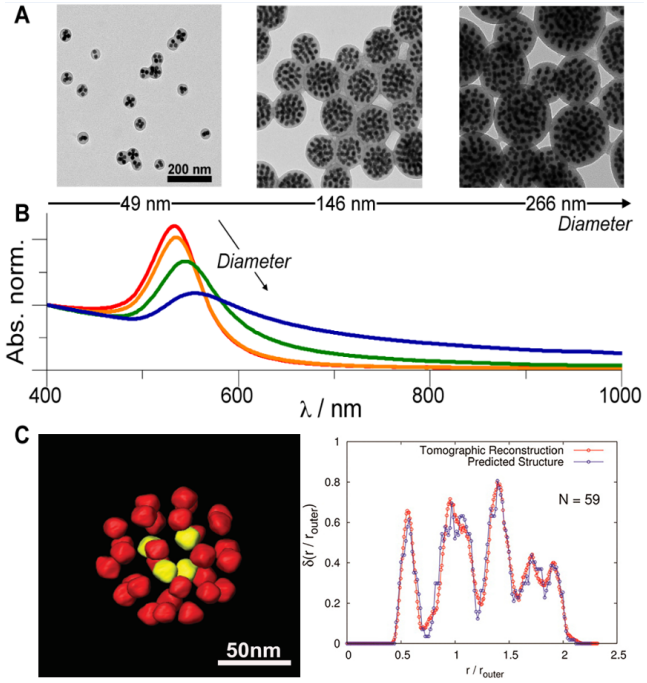

Figure 2. Clustering of gold nanoparticles. (A) TEM images for clusters of different size. (B) UV-Vis-NIR spectra of clusters showing redshift as cluster size increases. (C) Left: Electron tomography reconstruction of an individual cluster with shell-like structure. Center: Comparison of radial distribution functions. Right: computational reconstruction of the cluster. Adapted with permission from refs. 24 (Copyright (2012) American Chemical Society.) and 25 (Copyright (2014) American Chemical Society).

The morphology of the nanoparticle building blocks is also critical. For example, a rod-like shape gives rise to tunable plasmonic response, due to the possibility of exciting transverse and longitudinal surface plasmon resonances. Additionally, controlled assembly of nanorods would enable a unidirectional plasmon propagation, resulting in high performance platforms for enhanced spectroscopies. This was nicely demonstrated in a recent computational analysis of the SERS efficiency of random sub-monolayers of gold nanoparticles, as a function of nanoparticle morphology and coverage (interparticle distance).[26] As expected, monolayers of spheres and rods show increasing SERS intensity for higher coverage, with a sharp increase when hot spots arise, at surface coverage above 60%. The use of anisotropic nanoparticles is shown to provide an extra tool for design of optical platforms, *e.g.* nanorod monolayers performing better than nanospheres at longer wavelengths, due to coupling of longitudinal LSPR modes. However, the same study showed that nanostars with efficient response at single nanoparticle level do not perform much better at high coverage arrangements, which was also observed experimentally.[26,27] Dense monolayers of randomly distributed gold nanostars behave as an effective metamaterial, preventing the formation of hot spots. It should however be noted that, the absence of hot spots could also be attributed to the randomness of the array. Similar design criteria for the selection of nanoparticle shape can be translated to 3D arrangements.

Optical properties of 3D nanoparticle assemblies

Supercrystals have been obtained from colloidal dispersions of nanoparticles with various geometries, often resulting in large areas with a homogeneous optical response.[28,29,30] In an interesting development, 3D assemblies have also been obtained as well-defined pillars, even arranged at precise distances so that the plasmonic response is coupled to a collective photonic mode in the plane.[31] Anisotropic nanoparticles offer different orientation possibilities, *e.g.* defining areas within the 3D structure where the electric field is amplified, such as planes between ordered monolayers (**Figure 3**).[32,33]

Since hot spots in supercrystals are spatially confined at nanogaps between nanoparticles, the degree of order is a key parameter to define uniform interparticle distances and field enhancement. Taking Au nanorods as reference materials, large-scale simulations have shown than disordered nanostructures show broad absorption and scattering features similar to those of densely packed 2D nanoparticle films.[33] Calculations of SERS enhancement efficiency at different heights across the disordered structure demonstrated a significant decay when going deeper below the surface, *i.e.* gradual depletion of hot spots due to poor light penetration. Some analogies can be established between disordered 3D supercrystals and randomly deposited 2D nanoparticle films. In both cases, close packing and large areas are required to increase the density of hot spots resulting from plasmon coupling. It is however important to keep a balance between close packing (short interparticle distances), dimensions and sufficient interstitial space that allows molecular diffusion in between nanoparticles.[29]

Electromagnetic simulations for ordered nanorod supercrystals yield well-defined plasmonic features, which are strongly dependent on the alignment of the rods with the light polarization conditions.[33] The optical response of 3D nanorod supercrystals allows at certain wavelengths the generation of propagation modes, which are affected by the finite size of the supercrystal, producing photonic standing wave patterns which can penetrate through the whole structure of the supercrystal (**Figure 3**). Unlike disordered 3D structures, hot spots (corresponding to maxima of the standing waves) are distributed at different

resonant depths without depletion at deeper regions. In a more detailed experimental and theoretical analysis, it was found that an optimum number of monolayers can be identified,[34] but further work in this direction is required.[35]

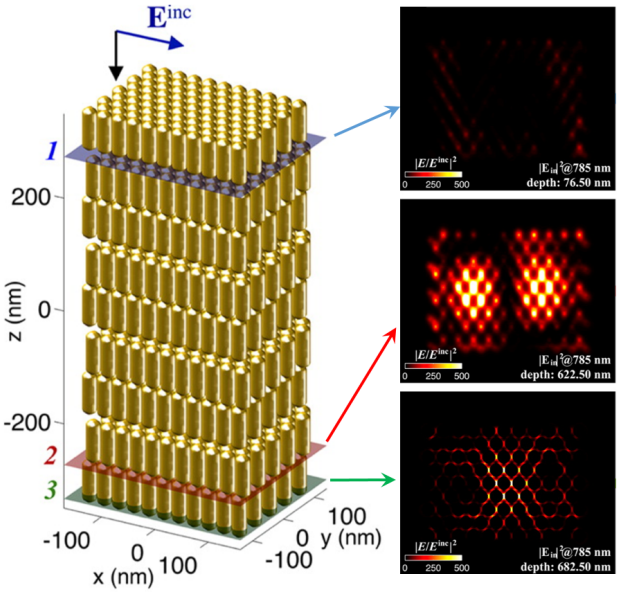

Figure 3. Scheme of a 3D supercrystal formed by vertically oriented nanorods and electric field intensity distribution at various interlayer planes. Adapted with permission from ref. 33. Copyright (2014) American Chemical Sociey.

Fabrication of plasmonic supercrystals.

Self-assembly can be considered as a thermodynamic process, directed by various types of interactions between the building blocks and the medium, which can be induced by external fields, or by using predefined templates.[36] The forces involved in these interactions can occur at interfaces (solid-liquid or liquid-air) or within a liquid phase.

Directed assembly. Focusing on plasmonic nanoparticles, the controlled assembly of nanoparticles in a liquid can give rise to the formation of colloidal crystals, which is often driven by specific interactions between capping ligands on nanoparticle surfaces. Macfarlane *et al.*[37] proposed the grafting of Au nanoparticles with polymer chains that terminate in functional groups capable of supramolecular binding. These non-covalent interactions enable programmable bonding that drives particle assembly. Alternatively, van der Boom *et al.*[38] studied the influence of the crystallinity of the building blocks and the nature of molecular cross-linkers as the key points to obtain Au superlattices. The most widely recognized approach to obtain nanoparticle superlattices is likely DNA-mediated assembly, first proposed by Mirkin and colleagues (**Figure 4**).[39] DNA hybridization guides nanoparticle assembly mimicking the atomic crystallization into Wulff polyhedra. DNA can even be used as a programmable ligand to obtain 2D and 3D mesoscale superlattices with either plasmonic or photonic properties, by controlling interparticle spacing.[40] The modular DNA design allows defining the distance between nanoparticles by expanding the rigid duplex region, as demonstrated by small-angle X-ray scattering (SAXS, **Figure 4C**). In a further advancement, Liu *et al.* demonstrated the possibility of fabricating 3D diamond superlattices using DNA origami as topological linkers.[41]

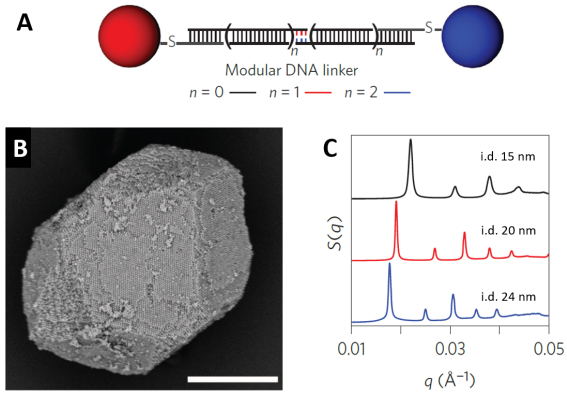

Figure 4. (A) Schematic view of DNA-directed assembly, where *n* represents a modular portion of the linker. (B) Representative SEM image of a supercrystal made of 20 nm Au nanoparticles. (C) SAXS plots for nanoparticle superlattices with varying interparticle distances (i.d.). Adapted with permission from refs. 39 (Copyright (2014) Springer Nature) and 40 (Copyright (2015) Springer Nature).

Nanoparticle crystallization can be favored by either drying or sedimentation effects involving two different media (solid-liquid or liquid-air interfaces). Different methodologies to obtain 3D nanoparticle assemblies including drop casting,[32,42] dip-coating,[43] layer-by-layer,[44] Langmuir-Blodgett,[45] spin-coating,[46] stamping,[28,47] or microfluidic pervaporation[29] have been reported. Often, the resulting 3D assembly is an array of randomly distributed nanoparticles with no control on morphology and dimensions, but careful control of certain parameters such as humidity, temperature or surface modification allows to obtain 3D hierarchical nanoparticle assemblies, *i.e.*, supercrystals.

Depletion forces. Alternatively, the synergy between depletion and electrostatic forces has been proposed as a driving force to induce the spontaneous assembly of anisotropic nanoparticles, such as gold nanorods or nanoplates, into colloidal crystals.[48] The presence of small nonadsorbing objects, such as micelles, in a colloidal dispersion, can induce depletion forces that favor nanoparticle assembly. Interestingly, it has been reported that the resulting lattice parameter can be tuned by controlling depletant concentration, temperature and ionic strength.[48] The combination of depletion forces with nanoscale geometrical features in anisotropic nanoparticles can also be used to direct the assembly into a variety of structures, as recently demonstrated for beveled gold triangular nanoprisms (**Figure 5A**).[49] In a different approach, Schroer *et al.*[50] explored the formation of gold nanoparticle supercrystals through a pressure-induced approach. Functionalization of the particles with poly(ethyleneglycol) (PEG) and a high salt concentration

were defined as pre-requisites to favor a liquid-to-solid phase transition, by applying hydrostatic pressure.

Drop casting. In general terms, we can claim that, drop-casting remains an ubiquitous strategy to fabricate nanoparticle assemblies. The technique literally comprises the evaporation of the solvent from a nanoparticle dispersion, deposited on a substrate. Solvent evaporation generates capillary forces and convective liquid flow, which kinetically induce the deposition of nanoparticles into 2D or 3D assemblies. The obtained nanostructures are however not necessarily ordered and usually present different particle density and organization at the borders (the well-known coffee-ring effect), due to Marangoni flows.[51] In an attempt to improve the quality of the resulting 3D assemblies in terms of size and order, various effects including the wettability of the substrate, the evaporation rate of the solvent[52,53] or the particle surface chemistry,[32] have been investigated. Guerrero-Martínez *et al.*[32] explored the replacement of cetyltrimethylammonium bromide (CTAB) on gold nanorods by a cationic gemini surfactant, which was expected to form stiffer bilayers connected to adjacent nanorods (**Figure 5B**). The quality of the 3D assembly could be further improved by controlling the temperature and humidity (20 ºC and 90%, respectively) to slow down the evaporation rate,[42] resulting in Au nanorod supercrystals with lateral dimensions up to 40 µm. A similar approach was followed by Liao *et al.*[52] to obtain micrometer-sized supercrystals from polyhedral gold nanoparticles as building blocks. Slow evaporation of the water droplet in a moist environment at 90 ºC resulted in supercrystals with different morphologies, defined by the building block morphology (**Figure 5C**). Interestingly, the obtained supercrystals were evenly distributed throughout the entire substrate surface originally covered by the droplet, rather than the usual coffee-ring assemblies.

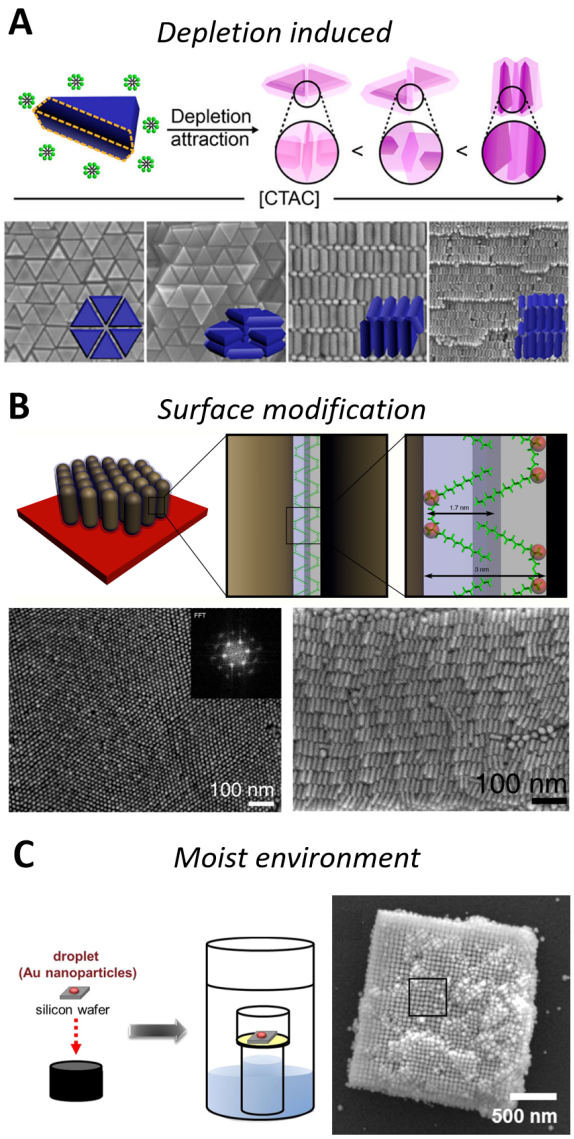

Figure 5. (A) Depletion induced assembly: surfactant (micellar) concentration dictates the obtained configuration. Reproduced with permission from ref. 49. Copyright (2017) American Chemical Society. (B) Gemini surfactant stabilized Au nanorods assembled into 3D standing superlattices upon drop casting. Adapted with permission from ref. 32. Copyright (2009) Wiley-VCH. (C) Schematic illustration of a setup used to assemble nanocrystals by drop-coating under temperature and humidity control, and SEM image of a cubic supercrystal obtained by assembly of Au nanocubes. Reproduced with permission from ref. 52. Copyright (2013) American Chemical Society.

Template-assisted method. The above methodologies do not allow for a precise control over the dimensions and morphology of the assemblies, as well as their position and organization over large areas. Such drawbacks have been overcome using template-assisted techniques,[28] by drying a highly concentrated nanoparticle dispersion between a hydrophilic substrate and a polydimethylsiloxane (PDMS) mold with holes that replicate the desired morphology. Careful removal of the mold resulted in regularly stamped assemblies on the substrate. This approach was used not only to form supercrystal arrays over macroscale areas, but

also with lattice parameters that can be tuned between 400 and 1600 nm, thereby providing control over the optical response (lattice plasmon modes), from the visible to the NIR.[31]

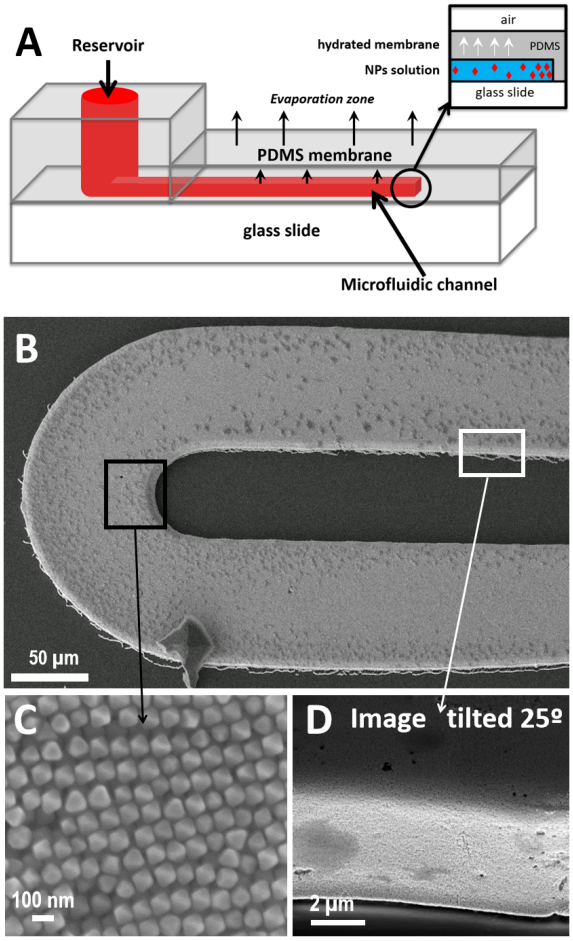

Figure 6. (A) Schematic illustration of an evaporation-based microfluidic cell used for 3D assembly. (B-D) SEM images showing a large 3D assembly (915 µm length, 100 µm width, 7 µm height). C and D were acquired from selected areas highlighted by the boxes. Adapted with permission from ref. 30. Copyright (2015) American Chemical Society.

Microfluidics-induced assembly. Although the template-assisted method allows a tight control over their morphology and organization, the fabrication of supercrystals over extended areas may be of interest for some applications. A recently developed microfluidic-induced approach was applied to obtain 3D assemblies with arbitrary morphologies and dimensions (from few microns to millimeters).[29,30] The method comprises a PDMS microfluidic evaporation cell made by standard soft photolithography, which is filled through capillary forces with a highly concentrated nanoparticle dispersion (**Figure 6A**). Subsequent evaporation of the solvent through the PDMS membrane drives the particles towards the end of the microchannel, where eventually the supercrystal nucleates and grows by continued nanoparticle deposition. **Figure 6B,C,D** illustrates the formation of a supercrystal from Au octahedra, spanning nearly 1 mm in length, 100 µm in width, and an average height of 7 µm.[30]

Applications

Precise control on the nanoparticle arrangement into larger ordered domains offers a unique opportunity to tune the magnetic, optical and electronic properties of individual building blocks, leading to novel collective properties within 3D superstructures, such as vibrational coherence, reversible metal-to-insulator transitions, enhanced p-type conductivity, spin-dependent electron transport, enhanced ferro- and ferrimagnetism, tunable magnetotransport and efficient charge transport.[54] We dedicate this section to some potential applications of 3D plasmonic supercrystals, which however remain mostly at the proof-of-concept level, meaning that application in real-world devices is still far from being fully implemented.

Following an unusual direction, Fan and co-workers[55] demonstrated the transformation of plasmonic supercrystals made of Au nanospheres into a 3D network of gold nanowires, through a stress induced phase transformation process. The gradual compression of the plasmonic supercrystal under isotropic hydrostatic pressure (below 8 GPa) allows a precise control of interparticle distances and therefore the modulation of plasmon coupling. At pressures above 8 GPa a nonhydrostatic pressure field is generated, driving adjacent particles to contact, coalescence and eventually sintering together into a 3D ordered nanowire network.[56] Such a pressure-dependent control over lattice structure provides a reversible process that can be used to understand fundamental collective physical properties and to get insight into novel electronic and photonic behaviors.[57]

The optical applications of 3D plasmonic supercrystals have still been insufficiently explored in the fields of metamaterials and sensing. A hierarchical 3D assembly made of densely packed "raspberry-like" plasmonic nanoparticles has been recently shown to behave as a metamaterial with strong isotropic artificial optical magnetism at visible frequencies.[58] Regarding optical sensing, Huang and co-workers[59] reported the application of polyhedral Au@Pd core@shell nanoparticle supercrystals to LSPR hydrogen sensing, taking advantage of the ability of Pd to dissociate molecular hydrogen and form palladium hydride.

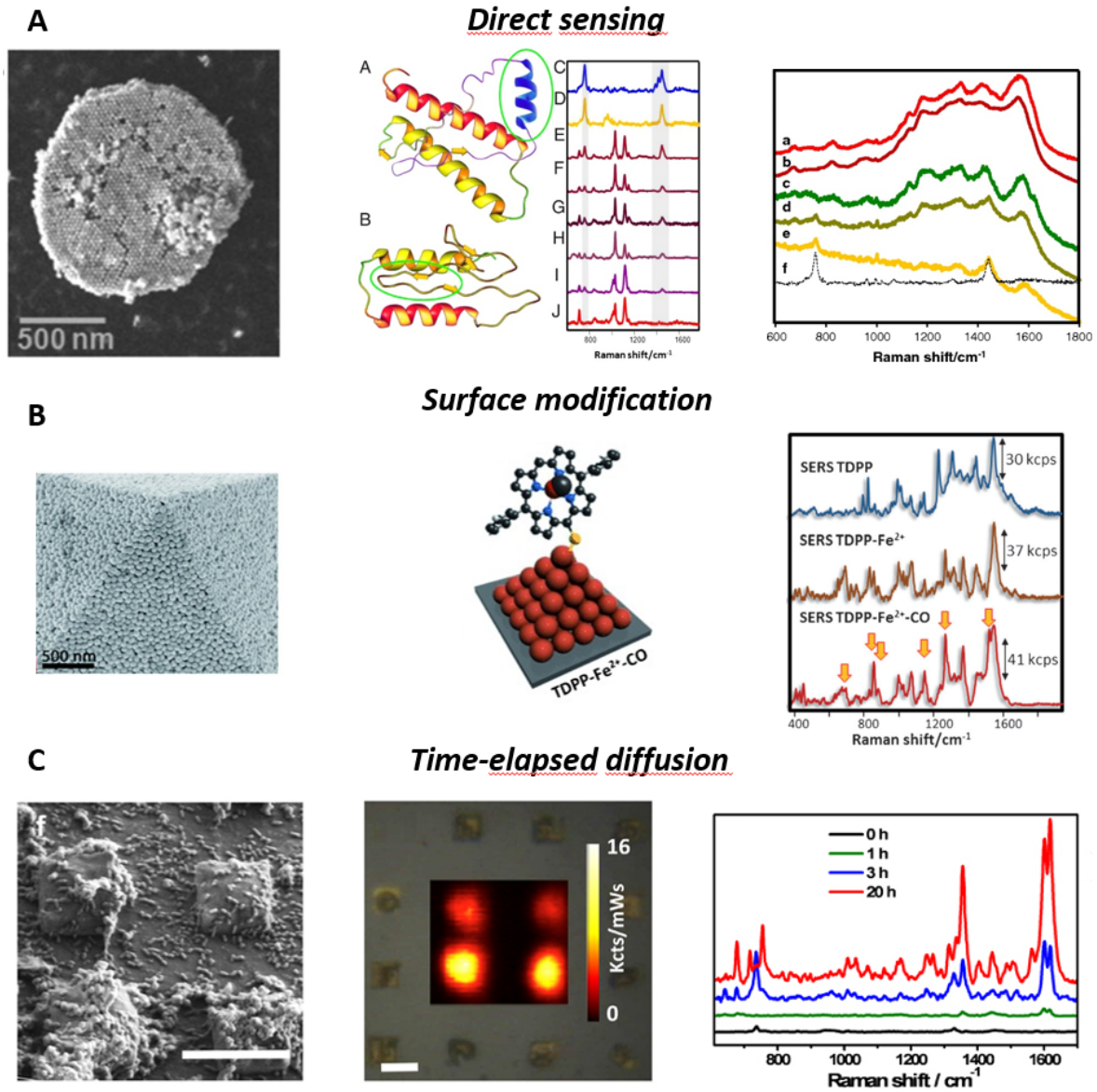

Figure 7. Examples of SERS-based sensing with plasmonic supercrystals. (A) *Direct sensing of scrambled prions:* SEM image of a gold nanorod supercrystal (left), representation of the prion mutation and its detection at 1% mutation (middle) and detection in human plasma after matrix subtraction (e,f) show the SERS spectra of scrambled prions in blood (right). Adapted with permission from ref. 60. Copyright (2011) National Academy of Sciences. (B) *CO detection via surface binding:* SEM image of a pyramidal supercrystal (left), schematic representation of the adsorption of an iron porphyrin with high CO affinity (middle), SERS spectra of free porphyrin, porphyrin coordinated to iron, and the iron porphyrin complexed with CO (right panel, the arrows highlight spectral changes after CO complexation). Adapted with permission from ref. 61. Copyright (2013) Wiley-VCH. (C) *Detection of the bacterial quorum sensing biomarker pyocyanin*: SEM images of silica-covered Au nanorod supercrystals colonized by *P. aeruginosa* (left), SERRS mapping of pyocyanin on the substrate (middle) and, SERRS spectra measured at selected times during the bacteria growth (right). Adapted with permission from ref. 12. Copyright (2016) Springer Nature.

On the other hand, the use of plasmonic supercrystals for SERS-based sensing is by far the most intensively investigated application. Plasmonic supercrystals can sustain standing waves, which are responsible for strong SERS enhancement.[33] The key factors behind the design of efficient SERS substrates not only rely on the morphology and composition of the building blocks, but also on their orientation within the nanostructure. For example, the SERS sensing capabilities of 3D nanorod superlattices change depending on the parallel or perpendicular orientation to the incoming light.[42] Supercrystals with both orientations were obtained by drop casting, using both Au and Au@Ag nanorods. The analysis revealed that the SERS enhancements at crystals of standing nanorods were 4-fold larger than those in lying structures, which was attributed to electric field transfer on the supercrystal. A further 4-fold increased SERS intensity was obtained for supercrystals comprising Au@Ag nanorods, due to the better plasmonic performance of silver with respect to gold.[62] It should be noted however, that silver based SERS substrates are less stable over time as they are prone to oxidation under ambient conditions.

Also using supercrystals of standing Au nanorods, Álvarez-Puebla *et al*.[60] demonstrated intense and homogeneous SERS response, together with high stability and reproducibility. The latter required removal of analytes using plasma etching the subsequent reuse of the plasmonic substrate. Plasmonic Au nanoparticle supercrystals thus offer the possibility of quantitative direct SERS detection or analysis in complex media. The great potential of these SERS substrates was explored toward the ultrasensitive detection of scrambled prions in serum and blood. The authors demonstrated that misfolded prions could be identified, even when their relative concentration was as low as 1% of the normal prion content, even at a total prion concentration of 0.1 nM, which is equivalent to 10 molecules per area sampled, that is, the zeptomolar regime (**Figure 7A**).

Alternatively, the surface of 3D supercrystals can be selectively modified with a highly active SERS molecule that can undergo vibrational changes upon interaction with the target analyte. This approach has been explored by Alba *et al*. for the reversible SERS-based detection of carbon monoxide in the atmosphere.[61] The sensor comprises a periodic array of pyramidal gold nanosphere assemblies, with side lengths of 4.4 μm and 3.0 μm height, fabricated by the template-assisted technique. The pyramidal superlattices with high plasmonic field accumulation, particularly at the tips, were functionalized with a thiolated iron porphyrin that shows high affinity and reversible binding to oxygen and carbon monoxide (**Figure 7B**). A detection-limit for CO between 1 and 100 ppm was reported. Additionally, the active sensor could be recovered within less than five minutes upon exposure to air, through oxygen mediated displacement, which enabled continuous monitoring of CO gas in the environment.

Although the SERS enhancement within a 3D plasmonic supercrystal is mostly concentrated at its external surface,[34] the above mentioned propagation modes would require strategies toward plasmonic supercrystals which permit the diffusion of the selected analyte from the external medium into the superlattice. Hamon et al.[11] proposed the simultaneous coating and infiltration of Au nanorod supercrystals with mesoporous silica, to enhance the stability of the supercrystal as well as improving molecular diffusion. The porosity of the silica matrix was shown to selectively allow the diffusion of small molecules and ions through the inner part of the plasmonic substrate. In this way, interferences from other molecules present in solution could be prevented. The results showed that silica infiltration improved the Raman enhancing properties of the plasmonic substrate up to 7-fold, suggesting a better accessibility to internal hot spots through the silica pores.[63] The molecular sieving capabilities of this nanostructured substrate were demonstrated for the *in situ*, label-free detection of pyocyanin, a bacterial quorum sensing (QS) signaling metabolite, in growing *Pseudomonas aeruginosa* biofilms and microcolonies (**Figure 7C**).[12] A limit of detection down to 10^{-14} M enabled ultrasensitive surface-enhanced resonance Raman scattering (SERRS) detection of QS events in low-density bacterial cultures, even at the initial hours of growth, as well as imaging of bacterial communication from undisturbed biological samples.

Conclusions and outlook

In this Account we focused on the fabrication of 3D plasmonic supercrystals, as well as relevant applications thereof. Even though it may be out of the scope here, we propose that further research on the comprehension of internal and external key forces involved in nanoparticle crystallization will be of great importance toward fabricating high performance supercrystals. Numerical simulations have predicted a great potential for monodisperse plasmonic nanoparticles of different size and shape in surface enhanced spectroscopies, when assembled into highly ordered 3D crystals. The localized surface plasmon modes of individual nanoparticles would then couple and originate collective modes that, given the finite size of the crystal, produce photonic standing waves penetrating the whole structure of the supercrystal. Therefore, not only the external surface of the assembly would display a high electric field enhancement but also its inner gaps and planes. Unfortunately, most of the proposed methodologies to obtain 3D assemblies do not favor subsequent infiltration of analytes, *e.g.* when dealing with SERS-based sensing applications. A challenging task is thus the development of novel assembly methods that overcome this limitation.

Another interesting field that requires development is the fabrication of heterogeneous assemblies through, *e.g.* the formation of binary systems with arbitrary combinations of nanoparticles. For example, the DNA-mediated assembly has been recently proposed as a general strategy to obtain binary heterogeneous systems involving gold nanoparticles and either quantum dots or magnetic nanoparticles.[64] Such studies should be extended to other types of particles such as upconverting nanoparticles or perovskites so that plasmon enhanced luminescence emission could be produced. Alternatively, starting from a closed packed binary superlattice, it is possible to obtain distinct nanoporous materials with the same chemical composition but different nanoscale architectures by the selective removal of one of their components, which envisions a wide range of optical, mechanical and catalytic properties.[45] Additionally, none of these heterogeneous systems has been explored in detail with other self-assembly approaches, such as the template-assisted or the microfluidic-induced pervaporation.

AUTHOR INFORMATION

Corresponding Authors

* J.P.-J. E-mail: juste@uvigo.es
L.M.L.-M. E-mail: llizmarzan@cicbiomagune.es.

ORCID

Daniel García-Lojo: 0000-0002-5477-6299

Sara Nuñez-Sánchez: 0000-0002-5435-6892

Sergio Gómez-Graña: 0000-0002-7736-051X

Marek Grzelczak: 0000-0002-3458-8450

Jorge Pérez-Juste: 0000-0002-4614-1699

Isabel Pastoriza-Santos: 0000-0002-1091-1364

Luis M. Liz-Marzán: 0000-0002-6647-1353

Biographical Information

Daniel García-Lojo is a Ph.D. candidate under the supervision of Jorge Pérez-Juste and Isabel Pastoriza-Santos at the University of Vigo. His research is focused on self-assembly of nanoparticles in microfluidic systems.

Sara Núñez-Sánchez holds a Ph.D. in Physics by the Universidad Autónoma de Madrid and the Spanish National Research Council (2010). She is currently working as postdoctoral researcher in the Colloid Chemistry Group at the University of Vigo.

Sergio Gómez-Graña has a Ph.D. from the University of Vigo (2013). He is currently a Juan de la Cierva Fellow at the University of Vigo.

Marek Grzelczak has a Ph.D. from the University of Vigo (2008). He is currently an Ikerbasque Associate Professor at the Donostia International Physics Center, San Sebastián.

Isabel Pastoriza-Santos has a Ph.D. from the University of Vigo (2001). She is currently an Associate Professor at the University of Vigo.

Jorge Pérez-Juste has a Ph.D. from the University of Vigo (1999). He is currently an Associate Professor at the University of Vigo.

Luis M. Liz-Marzán has a Ph.D. from the University of Santiago de Compostela (1992). He is currently an Ikerbasque Research Professor and Scientific Director of CIC biomaGUNE, in San Sebastián.

ACKNOWLEDGMENT

The authors acknowledge financial support by the Spanish Agencia Estatal de Investigación, Ministerio de Ciencia, Innovación y Universidades (Grants MAT2017-86659-R, MAT2016-77809-R and Juan de la Cierva fellowship FJCI to S. G.-G. and F.P.I. to D. G.-L.) and by the Fundación Ramón Areces (SERSforSafety).

REFERENCES

(1) Yang, P.; Arfaoui, I.; Cren, T.; Goubet, N.; Pileni, M. P. Unexpected Electronic Properties of Micrometer-Thick Supracrystals of Au Nanocrystals. *Nano Lett.* **2012**, *12*, 2051-2055.

(2) Boles, M. A.; Engel, M.; Talapin, D. V. Self-Assembly of Colloidal Nanocrystals: From Intricate Structures to Functional Materials. *Chem. Rev.* **2016**, *116*, 11220-11289.

(3) Sun, S. H.; Murray, C. B.; Weller, D.; Folks, L.; Moser, A. Monodisperse FePt nanoparticles and ferromagnetic FePt nanocrystal superlattices. *Science* **2000**, *287*, 1989-1992.

(4) Shevchenko, E. V.; Ringler, M.; Schwemer, A.; Talapin, D. V.; Klar, T. A.; Rogach, A. L.; Feldmann, J.; Alivisatos, A. P. Self-assembled binary superlattices of CdSe and Au nanocrystals and their fluorescence properties. *J. Am. Chem. Soc.* **2008**, *130*, 3274-3275.

(5) Bigioni, T. P.; Lin, X. M.; Nguyen, T. T.; Corwin, E. I.; Witten, T. A.; Jaeger, H. M. Kinetically driven self assembly of highly ordered nanoparticle monolayers. *Nat. Mater.* **2006**, *5*, 265-270.

(6) Bian, K. F.; Schunk, H.; Ye, D. M.; Hwang, A.; Luk, T. S.; Li, R. P.; Wang, Z. W.; Fan, H. Y. Formation of self-assembled gold nanoparticle supercrystals with facet-dependent surface plasmonic coupling. *Nat. Commun.* **2018**, *9*.

(7) Wang, C. Y.; Siu, C.; Zhang, J.; Fang, J. Y. Understanding the forces acting in self-assembly and the implications for constructing three-dimensional (3D) supercrystals. *Nano Res.* **2015**, *8*, 2445-2466.

(8) Sepulveda, B.; Angelome, P. C.; Lechuga, L. M.; Liz-Marzan, L. M. LSPR-based nanobiosensors. *Nano Today* **2009**, *4*, 244-251.

(9) Wang, Z. Y.; Zong, S. F.; Wu, L.; Zhu, D.; Cui, Y. P. SERS-Activated Platforms for Immunoassay: Probes, Encoding Methods, and Applications. *Chem. Rev.* **2017**, *117*, 7910-7963.

(10) Li, J. F.; Zhang, Y. J.; Ding, S. Y.; Panneerselvam, R.; Tian, Z. Q. Core-Shell Nanoparticle-Enhanced Raman Spectroscopy. *Chem. Rev.* **2017**, *117*, 5002-5069.

(11) Hamon, C.; Sanz-Ortiz, M. N.; Modin, E.; Hill, E. H.; Scarabelli, L.; Chuvilin, A.; Liz-Marzan, L. M. Hierarchical organization and molecular diffusion in gold nanorod/silica supercrystal nanocomposites. *Nanoscale* **2016**, *8*, 7914-7922.

(12) Bodelon, G.; Montes-Garcia, V.; Lopez-Puente, V.; Hill, E. H.; Hamon, C.; Sanz-Ortiz, M. N.; Rodal-Cedeira, S.; Costas, C.; Celiksoy, S.; Perez-Juste, I.; Scarabelli, L.; La Porta, A.; Perez-Juste, J.; Pastoriza-Santos, I.; Liz-Marzan, L. M. Detection and imaging of quorum sensing in Pseudomonas aeruginosa biofilm communities by surface-enhanced resonance Raman scattering. *Nat. Mater.* **2016**, *15*, 1203-1210.

(13) Alvarez-Puebla, R.; Liz-Marzan, L. M.; de Abajo, F. J. G. Light Concentration at the Nanometer Scale. *J. Phys. Chem. Lett.* **2010**, *1*, 2428-2434.

(14) Rodriguez-Gonzalez, B.; Burrows, A.; Watanabe, M.; Kiely, C. J.; Liz-Marzan, L. M. Multishell bimetallic AuAg nanoparticles: synthesis, structure and optical properties. *J. Mater. Chem.* **2005**, *15*, 1755-1759.

(15) Liz-Marzan, L. M. Tailoring surface plasmons through the morphology and assembly of metal nanoparticles. *Langmuir* **2006**, *22*, 32-41.

(16) Underwood, S.; Mulvaney, P. Effect of the Solution Refractive-Index on the Color of Gold Colloids. *Langmuir* **1994**, *10*, 3427-3430.

(17) Kumar, P. S.; Pastoriza-Santos, I.; Rodriguez-Gonzalez, B.; Garcia de Abajo, F. J.; Liz-Marzan, L. M. High-yield synthesis and optical response of gold nanostars. *Nanotechnology* **2008**, *19*, 015606.

(18) Rodriguez-Lorenzo, L.; Alvarez-Puebla, R. A.; Pastoriza-Santos, I.; Mazzucco, S.; Stephan, O.; Kociak, M.; Liz-Marzan, L. M.; de Abajo, F. J. G. Zeptomol Detection Through Controlled Ultrasensitive Surface-Enhanced Raman Scattering. *J. Am. Chem. Soc.* **2009**, *131*, 4616-4618.

(19) Pazos-Perez, N.; Wagner, C. S.; Romo-Herrera, J. M.; Liz-Marzan, L. M.; de Abajo, F. J. G.; Wittemann, A.; Fery, A.; Alvarez-Puebla, R. A. Organized Plasmonic Clusters with High Coordination Number and Extraordinary Enhancement in Surface-Enhanced Raman Scattering (SERS). *Angew. Chem., Int. Ed.* **2012**, *51*, 12688-12693.

(20) Taylor, R. W.; Esteban, R.; Mahajan, S.; Aizpurua, J.; Baumberg, J. J. Optimizing SERS from Gold Nanoparticle

Clusters: Addressing the Near Field by an Embedded Chain Plasmon Model. *J. Phys. Chem. C* **2016**, *120*, 10512-10522.

(21) Shiohara, A.; Novikov, S. M.; Solis, D. M.; Taboada, J. M.; Obelleiro, F.; Liz-Marzan, L. M. Plasmon Modes and Hot Spots in Gold Nanostar-Satellite Clusters. *J. Phys. Chem. C* **2015**, *119*, 10836-10843.

(22) Fernandez-Lopez, C.; Polavarapu, L.; Solis, D. M.; Taboada, J. M.; Obelleiro, F.; Contreras-Caceres, R.; Pastoriza-Santos, I.; Perez-Juste, J. Gold Nanorod-pNIPAM Hybrids with Reversible Plasmon Coupling: Synthesis, Modeling, and SERS Properties. *ACS Appl. Mater. Inter.* **2015**, *7*, 12530-12538.

(23) Rechberger, W.; Hohenau, A.; Leitner, A.; Krenn, J. R.; Lamprecht, B.; Aussenegg, F. R. Optical properties of two interacting gold nanoparticles. *Opt. Commun.*. **2003**, *220*, 137-141.

(24) Sanchez-Iglesias, A.; Grzelczak, M.; Altantzis, T.; Goris, B.; Perez-Juste, J.; Bals, S.; Van Tendeloo, G.; Donaldson, S. H.; Chmelka, B. F.; Israelachvili, J. N.; Liz-Marzan, L. M. Hydrophobic Interactions Modulate Self-Assembly of Nanoparticles. *ACS Nano* **2012**, *6*, 11059-11065.

(25) Galvan-Moya, J. E.; Altantzis, T.; Nelissen, K.; Peeters, F. M.; Grzelczak, M.; Liz-Marzan, L. M.; Bals, S.; Van Tendeloo, G. Self-Organization of Highly Symmetric Nanoassemblies: A Matter of Competition. *ACS Nano* **2014**, *8*, 3869-3875.

(26) Solis, D. M.; Taboada, J. M.; Obelleiro, F.; Liz-Marzan, L. M.; de Abajo, F. J. G. Optimization of Nanoparticle-Based SERS Substrates through Large Scale Realistic Simulations. *Acs Photonics* **2017**, *4*, 329-337.

(27) Serrano-Montes, A. B.; Langer, J.; Henriksen-Lacey, M.; de Aberasturi, D. J.; Solis, D. M.; Taboada, J. M.; Obelleiro, F.; Sentosun, K.; Bals, S.; Bekdemir, A.; Stellacci, F.; Liz-Marzan, L. M. Gold Nanostar-Coated Polystyrene Beads as Multifunctional Nanoprobes for SERS Bioimaging. *J. Phys. Chem. C* **2016**, *120*, 20860-20868.

(28) Hanske, C.; Gonzalez-Rubio, G.; Hamon, C.; Formentin, P.; Modin, E.; Chuvilin, A.; Guerrero-Martinez, A.; Marsal, L. F.; Liz-Marzan, L. M. Large-Scale Plasmonic Pyramidal Supercrystals via Templated Self-Assembly of Monodisperse Gold Nanospheres. *J. Phys. Chem. C* **2017**, *121*, 10899-10906.

(29) Angly, J.; Iazzolino, A.; Salmon, J. B.; Leng, J.; Chandran, S. P.; Ponsinet, V.; Desert, A.; Le Beulze, A.; Mornet, S.; Treguer-Delapierre, M.; Correa-Duarte, M. A. Microfluidic-Induced Growth and Shape-Up of Three-Dimensional Extended Arrays of Densely Packed Nanoparticles. *ACS Nano* **2013**, *7*, 6465-6477.

(30) Gomez-Grana, S.; Fernandez-Lopez, C.; Polavarapu, L.; Salmon, J. B.; Leng, J.; Pastoriza-Santos, I.; Perez-Juste, J. Gold Nanooctahedra with Tunable Size and Microfluidic-Induced 3D Assembly for Highly Uniform SERS-Active Supercrystals. *Chem. Mater.* **2015**, *27*, 8310-8317.

(31) Matricardi, C.; Hanske, C.; Garcia-Pomar, J. L.; Langer, J.; Mihi, A.; Liz-Marzan, L. M. Gold Nanoparticle Plasmonic Superlattices as Surface-Enhanced Raman Spectroscopy Substrates. *ACS Nano* **2018**, *12*, 8531-8539.

(32) Guerrero-Martinez, A.; Perez-Juste, J.; Carbo-Argibay, E.; Tardajos, G.; Liz-Marzan, L. M. Gemini-Surfactant-Directed Self-Assembly of Monodisperse Gold Nanorods into Standing Superlattices. *Angew. Chem., Int. Ed.* **2009**, *48*, 9484-9488.

(33) Solis, D. M.; Taboada, J. M.; Obelleiro, F.; Liz-Marzan, L. M.; de Abajo, F. J. G. Toward Ultimate Nanoplasmonics Modeling. *ACS Nano* **2014**, *8*, 7559-7570.

(34) Hamon, C.; Novikov, S. M.; Scarabelli, L.; Solis, D. M.; Altantzis, T.; Bals, S.; Taboada, J. M.; Obelleiro, F.; Liz-Marzan, L. M. Collective Plasmonic Properties in Few-Layer Gold Nanorod Supercrystals. *ACS Photonics* **2015**, *2*, 1482-1488.

(35) Wei, W.; Bai, F.; Fan, H. *Angew. Chem. Int. Ed.*, 10.1002/anie.201902620.

(36) Grzelczak, M.; Vermant, J.; Furst, E. M.; Liz-Marzan, L. M. Directed Self-Assembly of Nanoparticles. *ACS Nano* **2010**, *4*, 3591-3605.

(37) Zhang, J. Y.; Santos, P. J.; Gabrys, P. A.; Lee, S.; Liu, C.; Macfarlane, R. J. Self-Assembling Nanocomposite Tectons. *J. Am. Chem. Soc.* **2016**, *138*, 16228-16231.

(38) Boterashvili, M.; Shirman, T.; Popovitz-Biro, R.; Wen, Q.; Lahav, M.; van der Boom, M. E. Nanocrystallinity and direct cross-linkage as key-factors for the assembly of gold nanoparticle-superlattices. *Chem. Commun.* **2016**, *52*, 8079-8082.

(39) Auyeung, E.; Li, T. I. N. G.; Senesi, A. J.; Schmucker, A. L.; Pals, B. C.; de la Cruz, M. O.; Mirkin, C. A. DNA-mediated nanoparticle crystallization into Wulff polyhedra. *Nature* **2014**, *505*, 73-77.

(40) Ross, M. B.; Ku, J. C.; Vaccarezza, V. M.; Schatz, G. C.; Mirkin, C. A. Nanoscale form dictates mesoscale function in plasmonic DNA-nanoparticle superlattices. *Nat. Nanotechnol.* **2015**, *10*, 453-458.

(41) Liu, W. Y.; Tagawa, M.; Xin, H. L. L.; Wang, T.; Emamy, H.; Li, H. L.; Yager, K. G.; Starr, F. W.; Tkachenko, A. V.; Gang, O. Diamond family of nanoparticle superlattices. *Science* **2016**, *351*, 582-586.

(42) Gomez-Grana, S.; Perez-Juste, J.; Alvarez-Puebla, R. A.; Guerrero-Martinez, A.; Liz-Marzan, L. M. Self-Assembly of Au@Ag Nanorods Mediated by Gemini Surfactants for Highly Efficient SERS-Active Supercrystals. *Adv. Opt. Mater.* **2013**, *1*, 477-481.

(43) Huang, J. X.; Kim, F.; Tao, A. R.; Connor, S.; Yang, P. D. Spontaneous formation of nanoparticle stripe patterns through dewetting. *Nat. Mater.* **2005**, *4*, 896-900.

(44) Higashi, N.; Takagi, T.; Koga, T. Layer-by-layer fabrication of well-packed gold nanoparticle assemblies guided by a beta-sheet peptide network. *Polym. J.* **2010**, *42*, 95-99.

(45) Udayabhaskararao, T.; Altantzis, T.; Houben, L.; Coronado-Puchau, M.; Langer, J.; Popovitz-Biro, R.; Liz-Marzan, L. M.; Vukovic, L.; Kral, P.; Bals, S.; Klajn, R. Tunable porous nanoallotropes prepared by post-assembly etching of binary nanoparticle superlattices. *Science* **2017**, *358*, 514-518.

(46) Xia, D. Y.; Brueck, S. R. J. A facile approach to directed assembly of patterns of nanoparticles using interference lithography and spin coating. *Nano Lett.* **2004**, *4*, 1295-1299.

(47) Lee, Y. H.; Shi, W. X.; Lee, H. K.; Jiang, R. B.; Phang, I. Y.; Cui, Y.; Isa, L.; Yang, Y. J.; Wang, J. F.; Li, S. Z.; Ling, X. Y. Nanoscale surface chemistry directs the tunable assembly of silver octahedra into three two-dimensional plasmonic superlattices. *Nat. Commun.* **2015**, *6*, 6990.

(48) Young, K. L.; Jones, M. R.; Zhang, J.; Macfarlane, R. J.; Esquivel-Sirvent, R.; Nap, R. J.; Wu, J. S.; Schatz, G. C.; Lee, B.; Mirkin, C. A. Assembly of reconfigurable one-dimensional colloidal superlattices due to a synergy of fundamental nanoscale forces. *P. Natl. Acad. Sci. USA* **2012**, *109*, 2240-2245.

(49) Kim, J.; Song, X. H.; Ji, F.; Luo, B. B.; Ice, N. F.; Liu, Q. P.; Zhang, Q.; Chen, Q. Polymorphic Assembly from Beveled Gold Triangular Nanoprisms. *Nano Lett.* **2017**, *17*, 3270-3275.

(50) Schroer, M. A.; Lehmkuhler, F.; Moller, J.; Lange, H.; Grubel, G.; Schulz, F. Pressure-Stimulated Supercrystal Formation in Nanoparticle Suspensions. *J. Phys. Chem. Lett.* **2018**, *9*, 4720-4724.

(51) Deegan, R. D.; Bakajin, O.; Dupont, T. F.; Huber, G.; Nagel, S. R.; Witten, T. A. Capillary flow as the cause of ring stains from dried liquid drops. *Nature* **1997**, *389*, 827-829.

(52) Liao, C. W.; Lin, Y. S.; Chanda, K.; Song, Y. F.; Huang, M. H. Formation of Diverse Supercrystals from Self-Assembly of a Variety of Polyhedral Gold Nanocrystals. *J. Am. Chem. Soc.* **2013**, *135*, 2684-2693.

(53) Josten, E.; Wetterskog, E.; Glavic, A.; Boesecke, P.; Feoktystov, A.; Brauweiler-Reuters, E.; Rucker, U.; Salazar-Alvarez, G.; Bruckel, T.; Bergstrom, L. Superlattice growth and rearrangement during evaporation-induced nanoparticle self-assembly. *Sci. Rep.* **2017**, *7*.

(54) Nie, Z. H.; Petukhova, A.; Kumacheva, E. Properties and emerging applications of self-assembled structures made from inorganic nanoparticles. *Nat. Nanotechnol.* **2010**, *5*, 15-25.

(55) Wu, H. M.; Bai, F.; Sun, Z. C.; Haddad, R. E.; Boye, D. M.; Wang, Z. W.; Fan, H. Y. Pressure-Driven Assembly of Spherical Nanoparticles and Formation of 1D-Nanostructure Arrays. *Angew. Chem., Int. Ed.* **2010**, *49*, 8431-8434.

(56) Wu, H.; Bai, F.; Sun, Z. C.; Haddad, R. E.; Boye, D. M.; Wang, Z. W.; Huang, J. Y.; Fan, H. Y. Nanostructured Gold Architectures Formed through High Pressure-Driven Sintering of Spherical Nanoparticle Arrays. *J. Am. Chem. Soc.* **2010**, *132*, 12826-12828.

(57) Lu, Y.; Liu, G. L.; Lee, L. P. High-density silver nanoparticle film with temperature-controllable interparticle spacing for a tunable surface enhanced Raman scattering substrate. *Nano Lett.* **2005**, *5*, 5-9.

(58) Gomez-Grana, S.; Le Beulze, A.; Treguer-Delapierre, M.; Mornet, S.; Duguet, E.; Grana, E.; Cloutet, E.; Hadziioannou, G.; Leng, J.; Salmon, J. B.; Kravets, V. G.; Grigorenko, A. N.; Peyyety, N. A.; Ponsinet, V.; Richetti, P.; Baron, A.; Torrent, D.; Barois, P. Hierarchical self-assembly of a bulk metamaterial enables isotropic magnetic permeability at optical frequencies. *Mater. Horiz.* **2016**, *3*, 596-601.

(59) Chiu, C. Y.; Chen, C. K.; Chang, C. W.; Jeng, U. S.; Tan, C. S.; Yang, C. W.; Chen, L. J.; Yen, T. J.; Huang, M. H. Surfactant-Directed Fabrication of Supercrystals from the Assembly of Polyhedral Au-Pd Core-Shell Nanocrystals and Their Electrical and Optical Properties. *J. Am. Chem. Soc.* **2015**, *137*, 2265-2275.

(60) Alvarez-Puebla, R. A.; Agarwal, A.; Manna, P.; Khanal, B. P.; Aldeanueva-Potel, P.; Carbo-Argibay, E.; Pazos-Perez, N.; Vigderman, L.; Zubarev, E. R.; Kotov, N. A.; Liz-Marzan, L. M. Gold nanorods 3D-supercrystals as surface enhanced Raman scattering spectroscopy substrates for the rapid detection of scrambled prions. *P. Natl. Acad. Sci. USA* **2011**, *108*, 8157-8161.

(61) Alba, M.; Pazos-Perez, N.; Vaz, B.; Formentin, P.; Tebbe, M.; Correa-Duarte, M. A.; Granero, P.; Ferre-Borrull, J.; Alvarez, R.; Pallares, J.; Fery, A.; de Lera, A. R.; Marsal, L. F.; Alvarez-Puebla, R. A. Macroscale Plasmonic Substrates for Highly Sensitive Surface-Enhanced Raman Scattering. *Angew. Chem., Int. Ed.* **2013**, 52, 6459-6463.

(62) Cardinal, M. F.; Rodriguez-Gonzalez, B.; Alvarez-Puebla, R. A.; Perez-Juste, J.; Liz-Marzan, L. M. Modulation of Localized Surface Plasmons and SERS Response in Gold Dumbbells through Silver Coating. *J. Phys. Chem. C* **2010**, *114*, 10417-10423.

(63) Lopez-Puente, V.; Abalde-Cela, S.; Angelome, P. C.; Alvarez-Puebla, R. A.; Liz-Marzan, L. M. Plasmonic Mesoporous Composites as Molecular Sieves for SERS Detection. *J. Phys. Chem. Lett.* **2013**, *4*, 2715-2720.

(64) Zhang, Y. G.; Lu, F.; Yager, K. G.; van der Lelie, D.; Gang, O. A general strategy for the DNA-mediated self-assembly of functional nanoparticles into heterogeneous systems. *Nat. Nanotechnol.* **2013**, *8*, 865-872.

Table of Contents Graphic